ACCOUNTS
of chemical research

Transition-Metal-Centered Monocyclic Boron Wheel Clusters (M©B_n): A New Class of Aromatic Borometallic Compounds

CONSTANTIN ROMANESCU,[†] TIMUR R. GALEEV,[‡] WEI-LI LI,[†] ALEXANDER I. BOLDYREV,[*,‡] AND LAI-SHENG WANG[*,†]

[†]*Chemistry Department, Brown University, Providence, Rhode Island 02912, United States, and* [‡]*Department of Chemistry and Biochemistry, Utah State University, Logan, Utah 84322, United States*

RECEIVED ON MAY 18, 2012

CONSPECTUS

Atomic clusters have intermediate properties between that of individual atoms and bulk solids, which provide fertile ground for the discovery of new molecules and novel chemical bonding. In addition, the study of small clusters can help researchers design better nanosystems with specific physical and chemical properties. From recent experimental and computational studies, we know that small boron clusters possess planar structures stabilized by electron delocalization both in the σ and π frameworks. An interesting boron cluster is B_9^-, which has a D_{8h} molecular wheel structure with a single boron atom in the center of a B_8 ring. This ring in the D_{8h}-B_9^- cluster is connected by eight classical two-center, two-electron bonds. In contrast, the cluster's central boron atom is bonded to the peripheral ring through three delocalized σ and three delocalized π bonds. This bonding structure gives the molecular wheel double aromaticity and high electronic stability. The unprecedented structure and bonding pattern in B_9^- and other planar boron clusters have inspired the designs of similar molecular wheel-type structures. But these mimics instead substitute a heteroatom for the central boron.

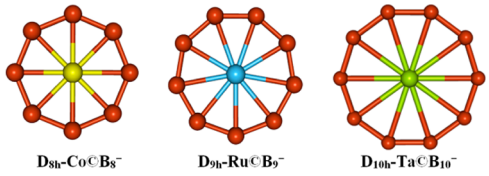

Through recent experiments in cluster beams, chemists have demonstrated that transition metals can be doped into the center of the planar boron clusters. These new metal-centered monocyclic boron rings have variable ring sizes, M©B_n and M©B_n^- with $n = 8-10$. Using size-selected anion photoelectron spectroscopy and *ab initio* calculations, researchers have characterized these novel borometallic molecules. Chemists have proposed a design principle based on σ and π double aromaticity for electronically stable borometallic cluster compounds, featuring a highly coordinated transition metal atom centered inside monocyclic boron rings. The central metal atom is coordinatively unsaturated in the direction perpendicular to the molecular plane. Thus, chemists may design appropriate ligands to synthesize the molecular wheels in the bulk. In this Account, we discuss these recent experimental and theoretical advances of this new class of aromatic borometallic compounds, which contain a highly coordinated central transition metal atom inside a monocyclic boron ring. Through these examples, we show that atomic clusters can facilitate the discovery of new structures, new chemical bonding, and possibly new nanostructures with specific, advantageous properties.

1. Introduction

The study of atomic clusters, with structures and properties intermediate between individual atoms and bulk solids, has a profound impact on our understanding of chemical bonding and the rational design of nanosystems with tailored physical and chemical properties.[1] Joint experimental and computational investigations over the past decade have demonstrated that negatively charged boron clusters (B_n^-) possess planar (2D) structures at least up to $n = 23$.[2−11] The propensity for planar structures in pure boron clusters, which can be traced to the electron-deficient character of the boron atoms, is in stark contrast with the three-dimensional (3D) structural motifs found in bulk boron and many solid boron derivatives. Even though the 2D−3D structural transition has been found to occur at $n = 16$ for cationic boron clusters[12] and $n = 20$ for neutral boron clusters,[6,13] this transition has not been found for anionic clusters. All planar boron clusters confirmed experimentally thus far consist of an outer ring, featuring strong two-center, two-electron (2c−2e) B−B bonds, and one or more inner atoms interacting with the peripheral ring via delocalized σ and π bonding.[3,6−11] To emphasize the role electron

Published on the Web 12/05/2012 www.pubs.acs.org/accounts
10.1021/ar300149a

delocalization plays in the stability of planar boron clusters, we note that the inner boron atoms in the anionic clusters ($n \leq 20$) are bonded to the outer ring almost exclusively by multicenter, two-electron bonds (nc−2e). One prototypical example is the circular B_{19}^- cluster (B©B_5©B_{13}),[14] which consists of two different delocalized π systems,[9] in addition to σ delocalized bonding. These delocalized bondings characterize the interactions between the central B atom and the middle B_5 ring and between the B_5 ring and the outer B_{13} ring. Interestingly, the inner B©B_5 moiety has been found to rotate almost freely inside the B_{13} outer ring, akin to an aromatic Wankel motor.[15] Similar fluxional behavior has also been found for the inner B_3 ring in the planar B_{13}^+ cluster, entirely owing to delocalized bonding between the B_3 unit and the outer B_{10} ring.[16]

The planar boron clusters that provided the inspiration for metal doping are the eight- and nine-atom boron clusters.[2,4] These two clusters stand out as perfectly symmetric molecular wheels: B_8^{2-} (D_{7h}) and B_9^- (D_{8h}), each with six σ and six π electrons conforming to the ($4N + 2$) Hückel rule for aromaticity.[2,4] Chemical bonding analyses using the adaptive natural density partitioning (AdNDP) method[17] confirmed that both clusters are doubly aromatic with unprecedented multicenter electron delocalization. It should be pointed out that the concept of double (σ and π) aromaticity was introduced for organic molecules previously.[18] However, attempts to substitute the central B atom with C to form carbon-centered wheel structures[19−21] were not successful and yielded only higher energy structures, because C avoids hypercoordination in B_xC_y clusters and prefers to participate in localized 2c−2e σ bonding on the periphery in the B−C mixed clusters.[22−24]

One interesting question was whether it would be possible to substitute the central B atom with a metal atom to create clusters with a central metal atom coordinated by a monocyclic boron ring (M©B_n).[14] It was shown that simple valence isoelectronic substitution by Al was not possible, only resulting in "umbrella"-type structures in AlB_7^- (C_{7v}) and AlB_8^- (C_{8v}),[25] in which Al interacts with a concave B_7 or B_8 unit primarily through ionic bonding and does not participate in delocalized bonding within the 2D boron frameworks. Similar ionic interactions have also been observed in larger AlB_n^- (n = 9−11) clusters.[26] Gold was also considered in a prior experiment, but it was found to form a covalent bond with a corner boron atom on the periphery of a planar B_{10} in AuB_{10}^-, whereas the D_{10h}-Au©B_{10}^- is a high-energy local minimum.[27]

Recently, we have successfully produced a series of transition-metal-centered boron rings in a supersonic cluster beam by laser vaporization of mixed boron−metal targets: Co©B_8^- and Ru©B_9^-,[28] Rh©B_9^- and Ir©B_9^-,[29] and Nb©B_{10}^- and Ta©B_{10}^-.[30] All these clusters have been shown to be the global minima on their respective potential energy curves. A design principle has been proposed for electronically stable M©B_n^{k-}-type compounds. These recent advances are discussed in this Account, and some future perspectives are outlined.

2. Experimental and Computational Methods

2.1. Cluster Generation and Photoelectron Spectroscopy. The experiment was done using a magnetic-bottle photoelectron spectroscopy (PES) apparatus equipped with a laser vaporization cluster source that was described in detail before.[31] Briefly, the metal-doped boron clusters were produced by laser vaporization of a disk target made of isotopically enriched ^{10}B or ^{11}B powder and the respective transition metals, balanced by Bi or Ag. The latter acted as target binders and also provided atomic anions, Bi^- or Ag^-, as calibrants for the photoelectron spectra. Depending on the mass and the isotope distributions of the metal dopant, different isotopically enriched boron was used to avoid mass overlaps between the metal-doped and pure boron clusters that were usually formed in larger amounts. The clusters were entrained in a He carrier gas seeded with 5% Ar and underwent a supersonic expansion to form a collimated cluster beam. Negatively charged clusters were extracted and analyzed with a time-of-flight mass spectrometer. An example of a mass spectrum for the $Nb_mB_n^-$ clusters produced by laser vaporization of a B/Nb target is shown in Figure S1, Supporting Information. The clusters of interest were mass-selected and decelerated before photodetachment by a laser beam at 193 nm (6.424 eV), 266 nm (4.661 eV), or 355 nm (3.496 eV). Photoelectrons were collected at nearly 100% efficiency by a magnetic bottle and analyzed in a 3.5 m long electron flight tube. The electron binding energy spectra were obtained by subtracting the electron kinetic energy spectra from the detachment photon energies. The resolution of the apparatus (ΔKE/KE) was better than 2.5%, that is, ~25 meV for 1 eV electrons.

2.2. Theoretical Calculations. Detailed information on the theoretical methods used for a given cluster is provided in the literature.[28−30] Briefly, the first step in understanding the photoelectron spectra and the structures of the doped boron clusters was the search for the global minimum using the coalescence-kick method[10] with density functional theory (DFT) calculations and small basis sets. The low-energy structures identified were further optimized using larger

basis sets. Vibrational frequency analyses were run to ensure that all the isomers were true minima on the respective potential energy surfaces. Finally, single point energies for the lowest isomers were calculated at CCSD(T), the "gold standard" of computational chemistry. Vertical detachment energies (VDEs) for the global minimum were calculated at DFT and CCSD(T) and were used to compare with the experimental data. When vibrational structures were resolved, the comparison of the experimental and theoretical vibrational frequencies provided further support to the identified global minimum. Chemical bonding was analyzed using molecular orbitals (MOs) and the AdNDP method,[17] which was particularly valuable for planar systems. The calculations were usually done using Gaussian 09,[32] except for those of $Ta©B_{10}^-$, which were done using the ADF program.[33] The MO visualization for the AdNDP analyses was done using Molekel 5.4.0.8.[34]

3. The Design Principle for Metal-Centered Boron Wheel Clusters ($M©B_n^{k-}$)

Despite numerous theoretical reports on molecular wheel-type clusters,[19−21] only the pure boron clusters, B_8^{2-} and B_9^-, with hepta- and octa-coordinated boron atoms were proven to be the global minima on their respective potential energy surfaces.[2,4] The chemical bonding of these two clusters involves classical 2c−2e bonds for the peripheral boron rings (seven for B_8^{2-} and eight for B_9^-) and six delocalized σ electrons and six delocalized π electrons. Thus, the bonding in these molecular wheels can be viewed as a monocyclic boron ring interacting with a central B atom entirely through delocalized bonds. Because the number of σ or π electrons each satisfies the $4N + 2$ Hückel rule for aromaticity, these molecular wheels are considered to be doubly aromatic. Thus, each peripheral B atom contributes two valence electrons to the 2c−2e bonds of the outer ring and one electron to the delocalized bonding between the outer ring and the central atom, whereas the central B atom contributes all three of its valence electrons to the delocalized bonding. Replacing the central B in B_8^{2-} by C would result in an isoelectronic D_{7h}-CB_7^-, which was found to be a local minimum.[22] In fact, all group-14 elements were found to give stable minima for D_{7h}-MB_7^- clusters.[21] However, C has been confirmed experimentally to avoid the central position, and the global minimum of CB_7^- has C_{2v} symmetry, in which the C atom is on the periphery.[22] The reason that C prefers the peripheral position is because C can form strong 2c−2e bonds, which is only possible on the periphery, whereas in the central position only delocalized multicenter bonding is possible. A D_{9h}-AlB_9^+ has been found to be a local minimum,[35] but we have shown that Al also does not favor the central planar position in AlB_9^-.[26a]

Once the main-group elements came out of favor as potential substituents for the central B atom to create molecular wheels, the focus of theoretical studies shifted to transition-metal-doped boron systems.[36−40] Two previous reports showed that D_{8h}-CoB_8^-, D_{9h}-FeB_9^-, and D_{8h}-FeB_8^{2-} were global minima, while a number of other transition metal doped boron rings (MB_n) with $n = 7-10$ were found to be only local minima.[36,38] Nucleus-independent chemical shift[41] calculations showed that all these clusters were highly aromatic. The introduction of the AdNDP method greatly simplified the bonding analysis and revealed that all planar wheel-type boron clusters featured double σ and π aromaticity.[40]

Based on the double aromaticity requirement, $(4N_\sigma + 2)$ delocalized σ electrons and $(4N_\pi + 2)$ delocalized π electrons to fulfill the Hückel aromaticity rule, a general electronic design principle has been proposed that involves the formal valence of the transition metal (x), the number of peripheral boron atoms (n), and the cluster's charge (k). To form electronically stable and doubly aromatic wheel-type clusters ($M^{(x)}©B_n^{k-}$), the design principle requires that the total number of bonding electrons present in the system, $3n + x + k$, participate in n 2c−2e B−B peripheral σ bonds and two sets of aromatic delocalized bonds (12 e for 6 σ and 6 π electrons), that is, $3n + x + k = 2n + 12$. In other words, for an electronically stable $M^{(x)}©B_n^{k-}$ cluster with double aromaticity, $n + x + k = 12$. For singly charged $M^{(x)}©B_n^-$ clusters ($k = 1$), $n + x = 11$. As shown below, in addition to the electron counting to satisfy double aromaticity, the ability of the central atom to form delocalized bonds and the favorable interactions between M and the B_n ring are also essential for the formation of the wheel structures.

However, geometric or steric considerations should probably limit the ring size to be at least seven atoms. For pure boron clusters, it was found that the B_7 cluster has a hexa-pyramidal structure,[5] which suggests that even the boron atom is too large to fit inside a B_6 ring. The smallest molecular wheel structure found experimentally is the D_{7h}-B_8^{2-} cluster,[4] while B_8^- has a slightly distorted planar structure with a D_{2h} symmetry due to the Jahn−Teller effect.[2] When applied to a hypothetical D_{7h}-$M©B_7^-$ cluster, the design principle requires a valence IV element. The formal satisfaction of the electron counting rules may not be sufficient to make the wheel structure the global minimum. For example, even though Au has the right valence to make an electronically stable $Au©B_{10}^-$ wheel, we have

shown that the wheel structure is not the global minimum for AuB_{10}^-,[27] because the Au 5d-AOs do not participate in bonding with the boron B_{10} ring.

4. Case Studies of M©B_n^- Molecular Wheels: From Theoretical Analyses to Experimental Discoveries

Clusters with high symmetry often have lower densities of energy levels as a result of degeneracy. Furthermore, chemical and thermodynamic stabilities are related to the electron affinity for open-shell neutral species or the energy gap between the highest occupied molecular orbital (HOMO) and the lowest unoccupied molecular orbital (LUMO) for closed-shell neutral species. Therefore, there are a number of signatures that can be readily recognized in PES spectra for highly stable and symmetric clusters. In the initial experimental effort, we screened a large number of transition-metal-doped boron clusters using PES to find clues about structural and electronic stabilities. To exemplify the approach, we show the PES data in Figure S2, Supporting Information for a set of ruthenium-doped boron clusters, RuB_n^- ($n = 3-10$). It can be clearly seen that RuB_9^- gives a relatively simple PES spectrum with a few narrow spectral features and an unusually high electron binding energies, providing hints for a highly stable and symmetric system. Similar screening experiments have been performed for many transition-metal-doped boron clusters, and a series of clusters have been discovered to form stable molecular wheel-type structures.[28−30]

4.1. M©B_8^- Molecular Wheels. When applied to a D_{8h}-M©B_8^- cluster, the design principle requires that the transition metal atom should contribute three valence electrons to delocalized bonding. Given the small size of the B_8 ring, the best candidate for such a cluster should be a 3d metal. Indeed, D_{8h}-CoB_8^- and -FeB_8^{2-} were calculated to be global minima.[36,38] CoB_8^- was the first D_{8h}-M©B_8^- molecular wheel characterized experimentally.[28] Figure 1 shows the PES spectra of CoB_8^- at two detachment photon energies. The global minimum D_{8h}-Co©B_8^- structure is shown in Figure 2A, which is similar to that reported in an earlier theoretical study.[36] To confirm that the D_{8h} structure is indeed the global minimum of CoB_8^-, we compared the computed VDEs with the experimental data and analyzed the vibrational structures resolved in the 266 nm spectrum. The calculated VDEs using both DFT and CCSD(T) methods showed good agreement with the experimental data.[28] To better understand the PES transitions and the structural changes that occur upon detachment of an electron from

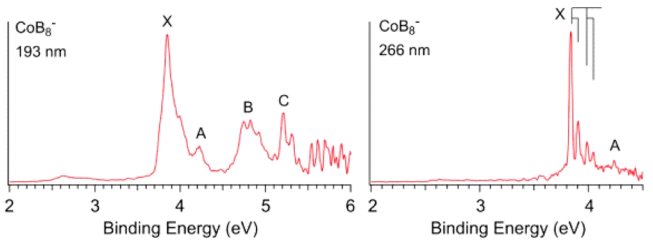

FIGURE 1. Photoelectron spectra of Co©B_8^- at 193 nm (left) and 266 nm (right).[28] The vertical lines in the 266 nm spectrum indicate vibrational structures. Reproduced from ref 28. Copyright 2011 Wiley.

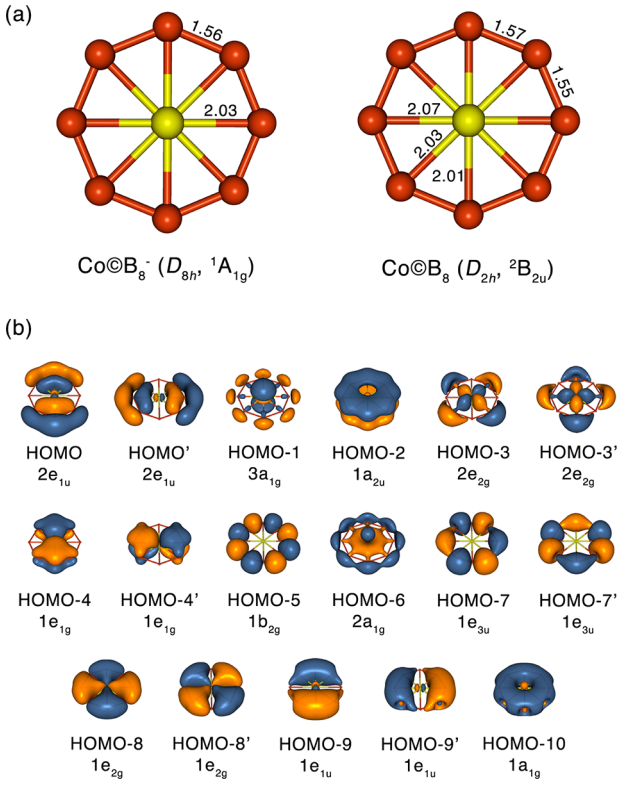

FIGURE 2. (A) Optimized structures for Co©B_8^- and Co©B_8 along with their point group symmetries and spectroscopic states (bond lengths are given in Å).[28] (B) Molecular orbitals and symmetries of Co©B_8^-. Reproduced from ref 28. Copyright 2011 Wiley.

Co©B_8^-, it is instructive to analyze the MOs of Co©B_8^- (Figure 2B). The HOMO of Co©B_8^- ($2e_{1u}$) is a degenerate σ orbital. Removal of one electron from the HOMO lifts the degeneracy, and the ensuing Jahn−Teller effect causes an in-plane distortion, reducing the symmetry of the neutral cluster to D_{2h} ($^2B_{2u}$) (Figure 2A). This geometry change is reflected in the resolved vibrational structures in the 266 nm spectrum (Figure 1), corresponding to two symmetric in-plane vibrational modes of the D_{2h}-Co©B_8 ground state. Good agreement was found between the calculated and the observed vibrational frequencies, lending further credence to the structural analyses.[28]

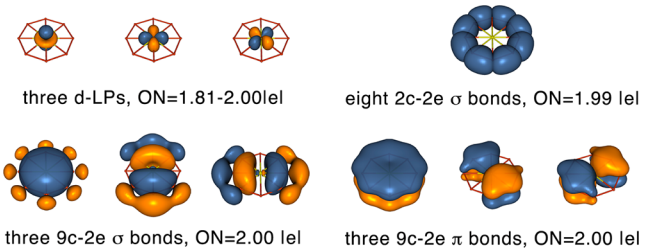

FIGURE 3. AdNDP analysis for Co©B_8^-.

Further chemical bonding analyses using AdNDP clearly revealed 3d lone pairs, localized 2c−2e B−B bonds, and delocalized 9c−2e σ and π bonds in Co©B_8^-, as shown in Figure 3. Co ($3d^74s^2$) has 9 valence electrons, resulting in a total of 34 valence electrons for CoB_8^-. It is in its +3 oxidation state in this case, and the AdNDP analyses revealed clearly three 3d lone-pairs (d_{z^2}, d_{xy}, $d_{x^2-y^2}$). The remaining 28 electrons form eight 2c−2e peripheral B−B bonds, three completely delocalized 9c−2e π-bonds, and three completely delocalized 9c−2e σ-bonds. The latter bonding features give rise to double aromaticity for Co©B_8^-, very similar to that in B_9^-.[2]

In addition to Co©B_8^-, we have also examined the isoelectronic RhB_8^- and IrB_8^- clusters (Figure S3, Supporting Information). Our preliminary analysis showed that these atoms are too large to fit inside a B_8-ring comfortably. As a consequence of the geometrical constraint, the metal atom is squeezed out of the plane slightly (~0.5 Å), distorting the RhB_8^- and IrB_8^- clusters to C_{8v} symmetry. Hence, D_{8h}-M©B_8^- type systems are probably the smallest boro-metallic molecular wheels.

4.2. M©B_9^- Molecular Wheels. For M©B_9^- systems, our design principle requires the central atom to be in its +2 oxidation state. The Fe-group elements are ideal to form closed-shell M©B_9^- clusters. Indeed, Fe©B_9^- was computed to be a stable minimum.[36−38,40] Our experimental PES spectra for Fe©B_9^- display broader features, indicating the possible presence of other low-lying isomers.[42] As shown in Figure S2, Supporting Information, RuB_9^- is the most promising example for a perfect D_{9h}-M©B_9^- cluster. The photoelectron spectra of RuB_9^- at 193 and 266 nm are displayed in Figure 4. The relatively simple PES pattern and unusually high electron binding energies suggested that RuB_9^- must be highly stable electronically and possess high symmetry. Our global optimization found indeed that the ground state of RuB_9^- possesses D_{9h} symmetry (Figure 5A). The MOs of the D_{9h}-Ru©B_9^- are shown in Figure 5B and can be used to understand the PES data.[28]

The HOMO of Ru©B_9^- is the nonbonding $4d_{z^2}$ orbital of Ru. Removal of one electron from this orbital, corresponding

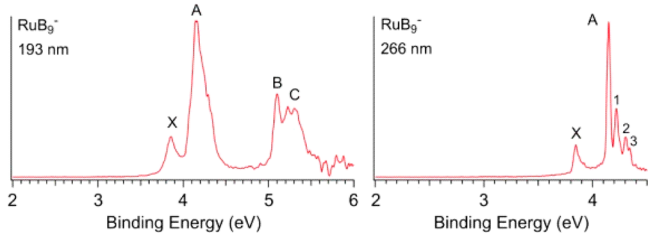

FIGURE 4. Photoelectron spectra of RuB_9^- at 193 nm (left) and 266 nm (right). The numbers in the 266 nm spectrum indicate vibrational structures. Reproduced from ref 28. Copyright 2011 Wiley.

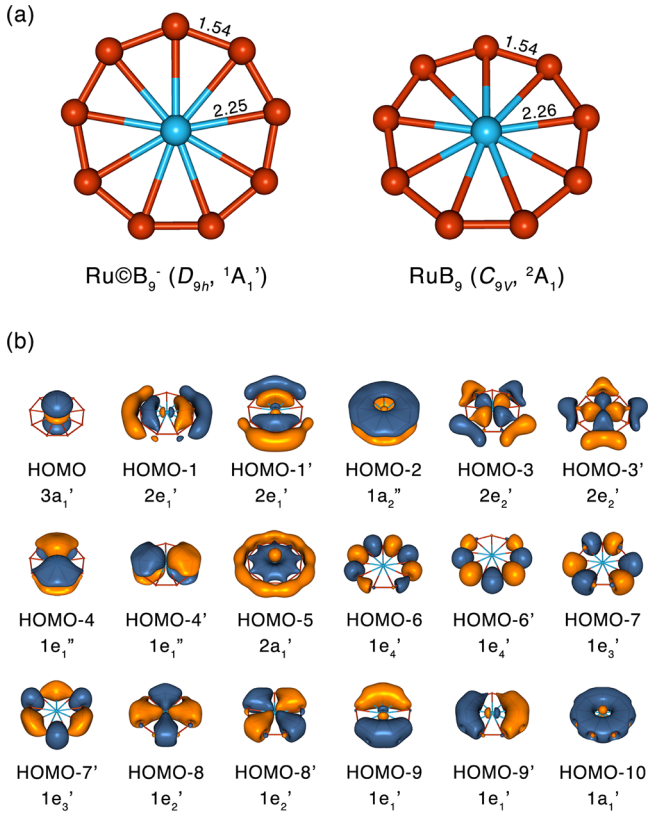

FIGURE 5. (A) Optimized structures for Ru©B_9^- and Ru©B_9 along with their point group symmetries and spectroscopic states (bond lengths are given in Å).[28] (B) Molecular orbitals and symmetries of Ru©B_9^-. Reproduced from ref 28. Copyright 2011 Wiley.

to the X band in the PES spectra (Figure 4), should not affect the peripheral B_9 ring. However, a very slight out-of-plane distortion of the Ru atom was observed from our geometrical optimization of the doublet ground state of the neutral, resulting in a C_{9v}-Ru©B_9 (Figure 5A).[28] The unresolved vibrational structure in the X band is consistent with the structural distortion: the vibrational frequency for the out-of-plane mode by Ru is computed to be only 36 cm^{-1}, which was too low to be resolved in our experiment. The HOMO − 1 of Ru©B_9^- is a doubly degenerate σ orbital, similar to the HOMO of Co©B_8^- (Figure 2B). Detachment of an electron

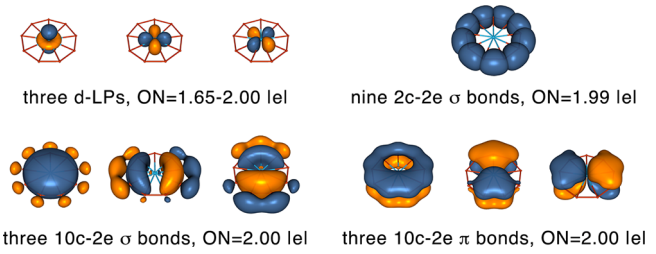

FIGURE 6. AdNDP analysis for Ru©B_9^-.

from this orbital corresponds to band A in the PES spectra (Figure 4). Indeed, we observed vibrational structures for this detachment band due to the expected Jahn–Teller effect, similar to the X band of Co©B_8^- (Figure 1). The calculated VDEs for the first four detachment channels of Ru©B_9^- are all in good agreement with the observed PES bands. The agreement between the theoretical and experimental results confirmed unequivocally that the global minimum of RuB_9^- is the D_{9h} molecular wheel.[28]

The AdNDP analysis shown in Figure 6 reveals that Ru©B_9^- is doubly aromatic with three σ and three π 10c–2e delocalized bonds consistent with the electronic requirement of our design principle, in addition to the nine 2c–2e B–B bonds for the B_9 ring and three 4d lone pairs.

4.3. Neutral M©B_9 Molecular Wheels. Our electronic design principle says $n + x = 12$ for doubly aromatic *neutral* clusters ($k = 0$). However, experimentally we can only study negatively charged species using PES of size-selected anions. For stable and closed-shell neutral M©B_n species, a large HOMO–LUMO gap is expected, which can be probed directly in the PES spectra of the corresponding anions. Based on the high stability of Ru©B_9^- discussed above, we expected that the isoelectronic neutral Rh©B_9 should be a good candidate as a stable neutral M©B_9 species. Indeed, we found that both Rh©B_9 and Ir©B_9 are highly stable and symmetric D_{9h} doubly aromatic species, as revealed in the PES spectra of their anions in Figure 7. The HOMO–LUMO gap defined by the X and A bands was measured to be 1.21 and 1.59 eV for Rh©B_9 and Ir©B_9, respectively.

Vibrational structures were resolved in the X band in each species (Figure 7B,D), suggesting that slight structural changes take place between the ground state of the anion and that of the neutral. Our structural optimizations showed that the global minima of Rh©B_9^- and Ir©B_9^- have C_{2v} symmetry due to the Jahn–Teller effects, whereas neutral Rh©B_9 and Ir©B_9 are perfect closed-shell molecular wheels with D_{9h} symmetry.[29]

4.4. M©B_{10}^- Molecular Wheels. The application of our design principle to a B_{10}-ring suggests that a transition metal

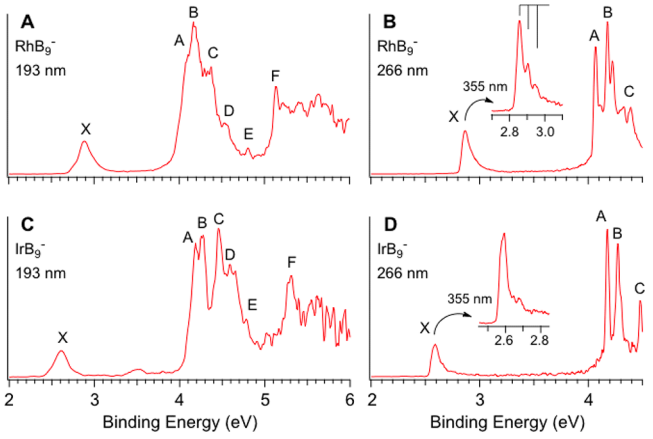

FIGURE 7. Photoelectron spectra of RhB_9^- and IrB_9^- at 355, 266, and 192 nm. The vertical lines in the 355 spectrum of RhB_9^- indicate vibrational structures. Reproduced from ref 29. Copyright 2012 American Chemical Society.

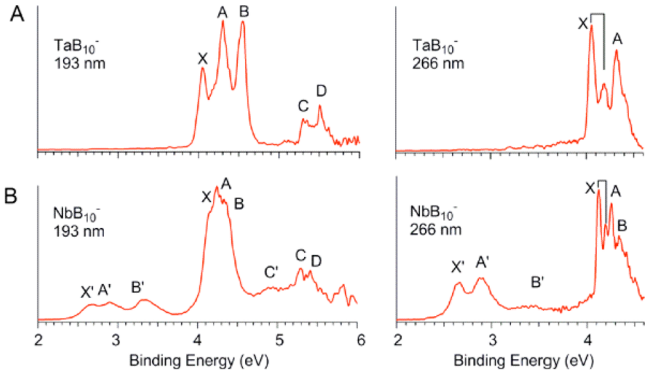

FIGURE 8. Photoelectron spectra of (A) TaB_{10}^- and (B) NbB_{10}^- at 193 and 266 nm. The vertical lines in the 266 nm spectra indicate vibrational structures. Reproduced from ref 30. Copyright 2012 Wiley.

with a valence of one is required to form stable M©B_{10}^- wheel structures ($x + n = 11$ for $k = 1$). However, previous experimental and computational results showed that the most promising candidate, Au©B_{10}^-, is more than 50 kcal/mol higher in energy relative to the global minimum structure, in which the Au atom is covalently bonded to a planar B_{10}^- cluster,[27] akin to a hydrogen atom.[43] The question was whether it would be possible to form metal-doped molecular wheels with B_{10} or larger boron rings.

Our extensive experimental screening of transition-metal-doped MB_n^- clusters led to a set of relatively simple PES spectra for TaB_{10}^-, as shown in Figure 8A.[30] The main PES features of the isoelectronic NbB_{10}^- cluster (Figure 8B) were observed to be similar to those of TaB_{10}^-, with additional low binding energy features (X′, A′, B′) probably due to a low-lying isomer. These observations prompted us to closely investigate the geometric structures and the bonding

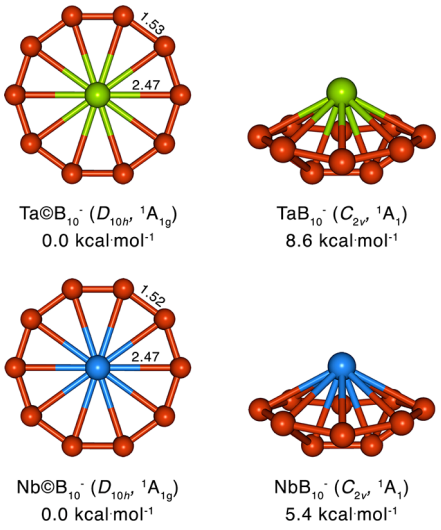

FIGURE 9. Optimized structures of the two lowest energy isomers of TaB_{10}^- and NbB_{10}^-, their point group symmetries, spectroscopic states, and relative energies (bond lengths are given in Å). Reproduced from ref 30. Copyright 2012 Wiley.

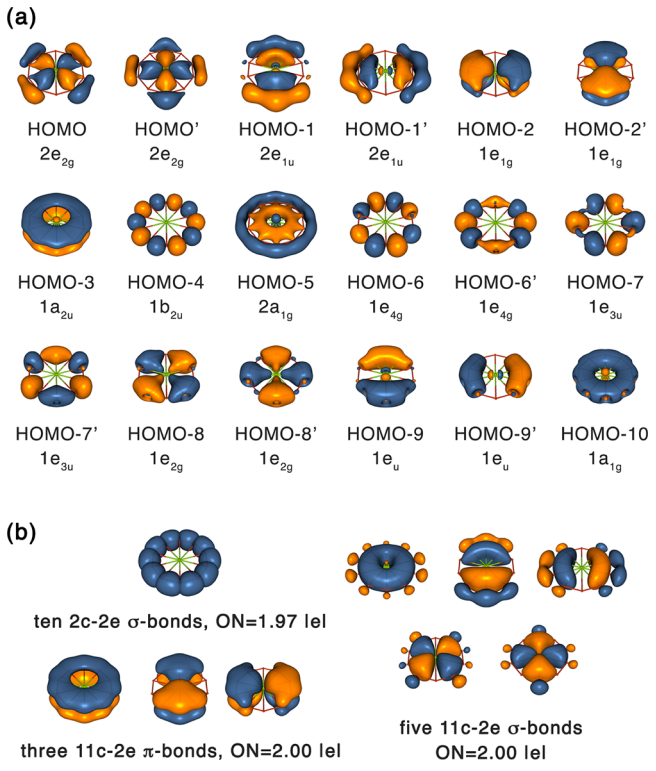

FIGURE 10. (A) Molecular orbitals and symmetries of $Ta©B_{10}^-$. (B) AdNDP analysis for $Ta©B_{10}^-$.

of these clusters. Global minimum searches for TaB_{10}^- revealed that its most stable structure possesses an unprecedented D_{10h} symmetry with a 3D "boat"-like isomer almost 9 kcal/mol higher in energy (Figure 9). The NbB_{10}^- cluster displays a similar set of structures, but its boat-like isomer is closer in energy to the global minimum D_{10h}-$Nb@B_{10}^-$ structure. Most importantly, the calculated VDEs of the D_{10h} global minimum are in good agreement with the observed PES features, whereas for NbB_{10}^- the calculated VDEs for the boat-like isomer were in good agreement with the low binding energy features. Clearly, under our experimental conditions, the boat isomer was weakly populated in the cluster beam of NbB_{10}^- because its energy was not too high relative to the global minimum molecular wheel.

We found that the relative stability of the D_{10h}-M©B_{10}^- wheel structure decreases going up the periodic table from M = Ta to V, as a result of the geometrical effects. For the valence isoelectronic VB_{10}^- cluster, we found that the wheel-type structure is only a high-lying isomer on the potential energy surface and is not present in the PES spectra.[44]

The chemical bonding analyses of the M©B_{10}^- molecular wheels are interesting. The MOs of $Ta©B_{10}^-$ (Figure 10A) indicate that there are six electrons in three completely delocalized π orbitals (HOMO-2, HOMO-2′, and HOMO-3) similar to the π electron system of the other metal-doped boron clusters. However, there are no localized 5d orbitals on the Ta center, that is, Ta is in its +5 oxidation state in $Ta©B_{10}^-$. The AdNDP analysis gives a more complete picture of the bonding situation in $Ta©B_{10}^-$, as shown in Figure 10B. There are 10 localized 2c−2e bonds responsible for the B_{10} ring and three totally delocalized π bonds. Interestingly, we observed *five* completely delocalized σ bonds with 10 electrons, in contrast to the usual three delocalized σ bonds observed in aromatic molecular-wheel-type planar boron or doped-boron clusters up to now. The 10 delocalized σ electrons also fulfill the $4N_\sigma + 2$ Hückel rule for aromaticity.[45] Thus, $Ta©B_{10}^-$ is doubly aromatic but with a total of 16 delocalized electrons. Therefore, the electronic design principle should be $x + 3n + k = 2n + 16$ or $x + n + k = 16$. For $Ta©B_{10}^-$, $x = 5$, $n = 10$, and $k = 1$. In other words, the 5d orbitals of Ta participate in the delocalized bonding with the peripheral B_{10}-ring. This bonding is critical for stabilizing the M©B_{10}^- molecular wheels. Since Au has a filled 5d shell that cannot effectively participate in bonding with the B_{10}-ring, the corresponding $Au©B_{10}^-$ molecular wheel is not stable.[27] In fact, even though the bonding in $Nb©B_{10}^-$ is similar to that in $Ta©B_{10}^-$, $Nb©B_{10}^-$ is less stable because the degree of the 4d bonding with the B_{10}-ring is weaker. The 3d-B_{10} bonding is even weaker, making $V©B_{10}^-$ much less stable.[44]

5. Conclusions and Perspective

We have discussed recent experimental and theoretical discoveries of a new class of aromatic borometallic

compounds, containing a highly coordinated central transition metal atom inside a monocyclic boron ring. Electronic design principles have been advanced that allow both rationalization of the stability of the D_{nh}-M©B_n^{k-} type molecular wheels and the prediction of new stable clusters. Research so far has focused on $n = 8-10$, which are the most promising size range. As concluded in a recent Perspective article by Heine and Merino,[46] "Are Ta©B_{10}^- and Nb©B_{10}^- the planar systems with the highest coordination number? We don't know." Indeed, we have not considered experimentally all the metal elements in the periodic table. The augmented design principle[45] for 6 delocalized π and 10 delocalized σ electrons predicts electronically stable M©B_{11}^- systems for valence IV metals. A more important and pertinent question is: can these molecular wheels be synthesized in bulk quantities and crystallized? Interestingly, planar monocyclic B_6 rings have been discovered recently as key structural building blocks in a multimetallic compound, $Ti_7Rh_4Ir_2B_8$.[47] A relevant question would be: what about transition metal doped boron rings in the bulk? On the other hand, because of the central position of the transition-metal atom in the M©B_n^{k-} molecular wheels, appropriate ligands may be conceived for coordination above and below the molecular plane, rendering chemical protection and allowing syntheses of this new class of novel borometallic complexes. The examples discussed in this Account demonstrate that atomic clusters remain a fertile field to discover new structures, new chemical bonding, and maybe new nanostructures with tailored properties.

The experimental work was supported by NSF (Grant DMR-0904034 to L.S.W.) and the computational work was also supported by NSF (Grant CHE-1057746 to A.I.B.). Computer times from the Centers for High Performance Computing at the University of Utah and Utah State University are gratefully acknowledged.

Supporting Information. Complete ref 32, mass spectrum of $Nb_mB_n^-$, and the comparison of the photoelectron spectra of CoB_8^-, RuB_8^-, and IrB_8^-. This information is available free of charge via the Internet at http://pubs.acs.org.

BIOGRAPHICAL INFORMATION

Constantin Romanescu received his Ph.D. degree in physical chemistry from Queen's University at Kingston, Ontario, Canada. After a postdoctoral stay at SRI International, Menlo Park, California, he joined Prof. Wang's group at Brown University as a Postdoctoral Research Associate in 2010.

Timur R. Galeev obtained his B.S. (2006) and M.S. (2008) in chemistry from Peoples' Friendship University of Russia, Moscow. He worked as a synthetic organic chemist at the Chemical Diversity Research Institute, Khimki, Russia, before joining Professor Boldyrev's group in 2010 to pursue his Ph.D. degree in theoretical physical chemistry.

Wei-Li Li received her B.S. degree in chemical physics from the University of Science and Technology of China in 2009. She is currently a Ph.D. student in Prof. Wang's group focusing on experimental studies of size-selected nanoclusters.

Alexander I. Boldyrev received his B.S./M.S. in chemistry from Novosibirsk University, his Ph.D, in physical chemistry from Moscow State University, and his Dr. Sci. in chemical physics from Moscow Physico-Chemical Institute. He worked as a leading researcher at the Institute of New Chemical Problems of the USSR Academy of Sciences, Chernogolovka, and at the Institute of Chemical Physics of the USSR Academy of Sciences, Moscow. He is currently professor of chemistry at Utah State University. His current scientific interest is the development of chemical bonding models capable of predicting the structure, stability, and other molecular properties of pure and mixed main group atomic clusters, with the most recent foray into transition metal chemical compounds and novel 2D materials.

Lai-Sheng Wang received his B.S. degree from Wuhan University in China and his Ph.D. from the University of California at Berkeley. After a postdoctoral stay at Rice University, he took a joint position between Washington State University and Pacific Northwest National Laboratory, then accepted an appointment as Professor of Chemistry at Brown University in 2009. His research group focuses on the investigation of the fundamental behaviors of nanoclusters using photoelectron spectroscopy and computational tools, as well as spectroscopic studies of free multiply charged anions and complex solution-phase molecules using electrospray ionization.

FOOTNOTES

*To whom correspondence should addressed. E-mail addresses: a.i.boldyrev@usu.edu; lai-sheng_wang@brown.edu.

The authors declare no competing financial interest.

REFERENCES

1 Fehlner, T. P.; Halet, J. F.; Saillard, J. Y. *Molecular Clusters: A Bridge to Solid-State Chemistry*; Cambridge University Press: Cambridge, U.K., 2007.

2 Zhai, H. J.; Alexandrova, A. N.; Birch, K. A.; Boldyrev, A. I.; Wang, L. S. Hepta- and octacoordinate boron in molecular wheels of eight- and nine-atom boron clusters: Observation and confirmation. *Angew. Chem., Int. Ed.* **2003**, *42*, 6004–6008.

3 Zhai, H. J.; Kiran, B.; Li, J.; Wang, L. S. Hydrocarbon analogues of boron clusters - planarity aromaticity and antiaromaticity. *Nat. Mater.* **2003**, *2*, 827–833.

4 Alexandrova, A. N.; Zhai, H. J.; Wang, L. S.; Boldyrev, A. I. Molecular wheel B_8^{2-} as a new inorganic ligand. Photoelectron spectroscopy and ab initio characterization of LiB_8^-. *Inorg. Chem.* **2004**, *43*, 3552–3554.

5 Alexandrova, A. N.; Boldyrev, A. I.; Zhai, H. J.; Wang, L. S. Electronic structure, isomerism, and chemical bonding in B_7^- and B_7. *J. Phys. Chem. A* **2004**, *108*, 3509–3517.

6 Kiran, B.; Bulusu, S.; Zhai, H. J.; Yoo, S.; Zeng, X. C.; Wang, L. S. Planar-to-tubular structural transition in boron clusters: B_{20} as the embryo of single-walled boron nanotubes. *Proc. Natl. Acad. Sci. U.S.A.* **2005**, *102*, 961–964.

7 Alexandrova, A. N.; Boldyrev, A. I.; Zhai, H. J.; Wang, L. S. All-boron aromatic clusters as potential new inorganic ligands and building blocks in chemistry. *Coord. Chem. Rev.* **2006**, *250*, 2811–2866.

8 Sergeeva, A. P.; Zubarev, D. Y.; Zhai, H. J.; Boldyrev, A. I.; Wang, L. S. Photoelectron spectroscopic and theoretical study of B_{16}^- and B_{16}^{2-}: An all-boron naphthalene. *J. Am. Chem. Soc.* **2008**, *130*, 7244–7246.

9 Huang, W.; Sergeeva, A. P.; Zhai, H. J.; Averkiev, B. B.; Wang, L. S.; Boldyrev, A. I. A concentric planar doubly π-aromatic B_{19}^- cluster. *Nat. Chem.* **2010**, *2*, 202–206.

10 Sergeeva, A. P.; Averkiev, B. B.; Zhai, H. J.; Boldyrev, A. I.; Wang, L. S. All-boron analogues of aromatic hydrocarbons: B_{17}^- and B_{18}^-. *J. Chem. Phys.* **2011**, *134*, No. 224304.

11 (a) Piazza, Z. A.; Li, W. L.; Romanescu, C.; Sergeeva, A. P.; Wang, L. S.; Boldyrev, A. I. A photoelectron spectroscopy and ab initio study of B_{21}^-: Negatively charged boron clusters continue to be planar at 21. *J. Chem. Phys.* **2012**, *136*, No. 104310. (b) Sergeeva, A. P.; Piazza, Z. A.; Romanescu, C.; Li, W. L.; Boldyrev, A. I.; Wang, L. S. B_{22}^- and B_{23}^-: All-boron analogues of anthracene and phenanthrene. *J. Am. Chem. Soc.* **2012**, *134*, 18065–18073.

12 Oger, E.; Crawford, N. R. M.; Kelting, R.; Weis, P.; Kappes, M. M.; Ahlrichs, R. Boron cluster cations: Transition from planar to cylindrical structures. *Angew. Chem., Int. Ed.* **2007**, *46*, 8503–8506.

13 Tai, T. B.; Tam, N. M.; Nguyen, M. T. Structure of boron clusters revisited, B_n with n = 14−20. *Chem. Phys. Lett.* **2012**, *530*, 71–76.

14 The © symbol is used to denote planar atom-centered wheel type structures. It was first suggested in ref **28**.

15 Jimenez-Halla, J. O. C.; Islas, R.; Heine, T.; Merino, G. B_{19}^-: An aromatic Wankel motor. *Angew. Chem., Int. Ed.* **2010**, *49*, 5668–5671.

16 Martinez-Guajardo, G.; Sergeeva, A. P.; Boldyrev, A. I.; Heine, T.; Ugalde, J. M.; Merino, G. Unraveling phenomenon of internal rotation in B_{13}^+ through chemical bonding analysis. *Chem. Commun.* **2011**, *47*, 6242–6244.

17 Zubarev, D. Y.; Boldyrev, A. I. Developing paradigms of chemical bonding: Adaptive natural density partitioning. *Phys. Chem. Chem. Phys.* **2008**, *10*, 5207–5217.

18 (a) Chandrasekhar, J.; Jemmis, E. D.; Schleyer, P. v. R. Double aromaticity-aromaticity in orthogonal planes-3,5-dehydrophenyl cation. *Tetrahedron Lett.* **1979**, *39*, 3707–3710. (b) McEwen, A. B.; Schleyer, P. v. R. In-plane aromaticity and trishomoaromaticity: A computational evaluation. *J. Org. Chem.* **1986**, *51*, 4357–4368. (c) Schleyer, P. v. R.; Jiao, H.; Glukhovtsev, M. N.; Chandrasekhar, J.; Kraka, E. Double aromaticity in the 3,5-dehydrophenyl cation and in cyclo[6]carbon. *J. Am. Chem. Soc.* **1994**, *116*, 10129–10134.

19 (a) Exner, K.; Schleyer, P. v. R. Planar hexacoordinate carbon: A viable possibility. *Science* **2000**, *290*, 1937–1940. (b) Wang, Z. X.; Schleyer, P. v. R. Construction principles of "hyparenes": Families of molecules with planar pentacoordinate carbons. *Science* **2001**, *292*, 2465–2469.

20 Erhardt, S.; Frenking, G.; Chen, Z. F.; Schleyer, P. v. R. Aromatic boron wheels with more than one carbon atom in the center: C_2B_8, $C_3B_9^{3+}$, and $C_5B_{11}^+$. *Angew. Chem., Int. Ed.* **2005**, *44*, 1078–1082.

21 Islas, R.; Heine, T.; Ito, K.; Schleyer, P. v. R.; Merino, G. Boron rings enclosing planar hypercoordinate group 14 elements. *J. Am. Chem. Soc.* **2007**, *129*, 14767–14774.

22 Wang, L. M.; Huang, W.; Averkiev, B. B.; Boldyrev, A. I.; Wang, L. S. CB_7^-: Experimental and theoretical evidence against hypercoordinate planar carbon. *Angew. Chem., Int. Ed.* **2007**, *46*, 4550–4553.

23 Averkiev, B. B.; Zubarev, D. Y.; Wang, L. M.; Huang, W.; Wang, L. S.; Boldyrev, A. I. Carbon avoids hypercoordination in CB_6^-, CB_6^{2-}, and $C_2B_5^-$ planar carbon-boron clusters. *J. Am. Chem. Soc.* **2008**, *130*, 9248–9250.

24 Galeev, T. R.; Ivanov, A. S.; Romanescu, C.; Li, W. L.; Bozhenko, K. V.; Wang, L. S.; Boldyrev, A. I. Molecular wheel to monocyclic ring transition in boron-carbon mixed clusters $C_2B_6^-$ and $C_3B_5^-$. *Phys. Chem. Chem. Phys.* **2011**, *13*, 8805–8810.

25 Galeev, T. R.; Romanescu, C.; Li, W. L.; Wang, L. S.; Boldyrev, A. I. Valence isoelectronic substitution in the B_8^- and B_9^- molecular wheels by an Al dopant atom: Umbrella-like structures of AlB_7^- and AlB_8^-. *J. Chem. Phys.* **2011**, *135*, No. 104301.

26 (a) Li, W. L.; Romanescu, C.; Galeev, T. R.; Wang, L. S.; Boldyrev, A. I. Aluminum avoids the central position in AlB_9^- and AlB_{10}^-: Photoelectron spectroscopy and ab initio study. *J. Phys. Chem. A* **2011**, *115*, 10391–10397. (b) Romanescu, C.; Sergeeva, A. P.; Li, W. L.; Boldyrev, A. I.; Wang, L. S. Planarization of B_7^- and B_{12}^- clusters by isoelectronic substitution: AlB_6^- and AlB_{11}^-. *J. Am. Chem. Soc.* **2011**, *133*, 8646–8653.

27 Zhai, H. J.; Miao, C. Q.; Li, S. D.; Wang, L. S. On the analogy of B−BO and B−Au chemical bonding in $B_{11}O^-$ and $B_{10}Au^-$ clusters. *J. Phys. Chem. A* **2010**, *114*, 12155–12161.

28 Romanescu, C.; Galeev, T. R.; Li, W. L.; Boldyrev, A. I.; Wang, L. S. Aromatic metal-centered monocyclic boron rings: $Co©B_8^-$ and $Ru©B_9^-$. *Angew. Chem., Int. Ed.* **2011**, *50*, 9334–9337.

29 Li, W. L.; Romanescu, C.; Galeev, T. R.; Piazza, Z. A.; Boldyrev, A. I.; Wang, L. S. Transition-metal-centered nine-membered boron rings: $M©B_9$ and $M©B_9^-$ (M = Rh, Ir). *J. Am. Chem. Soc.* **2012**, *134*, 165–168.

30 Galeev, T. R.; Romanescu, C.; Li, W. L.; Wang, L. S.; Boldyrev, A. I. Observation of the highest coordination number in planar species: Decacoordinated $Ta©B_{10}^-$ and $Nb©B_{10}^-$ anions. *Angew. Chem., Int. Ed.* **2012**, *51*, 2101–2105.

31 Wang, L. S.; Cheng, H. S.; Fan, J. W. Photoelectron spectroscopy of size-selected transition-metal clusters: Fe_n^-, n = 3−24. *J. Chem. Phys.* **1995**, *102*, 9480–9493.

32 Frisch, M. J. et al. Gaussian 09, Rev. B.01. Gaussian Inc.: Wallingford, CT, 2009.

33 ADF 2010. SCM, Theoretical Chemistry, Vrije Universiteit: Amsterdam, the Netherlands, 2010.

34 Varetto, U. Molekel 5.4.0.8. Swiss National Supercomputing Centre: Manno (Switzerland), 2009.

35 Averkiev, B. B.; Boldyrev, A. I. Theoretical design of planar molecules with a nona- and decacoordinate central atom. *Russ. J. Gen. Chem.* **2008**, *78*, 769–773.

36 Ito, K.; Pu, Z.; Li, Q. S.; Schleyer, P. v. R. Cyclic boron clusters enclosing planar hypercoordinate cobalt, iron, and nickel. *Inorg. Chem.* **2008**, *47*, 10906–10910.

37 Luo, Q. O. Boron rings containing planar octa- and enneacoordinate cobalt, iron and nickel metal elements. *Sci. China, Ser. B: Chem.* **2008**, *51*, 607–613.

38 Pu, Z. F.; Ito, K.; Schleyer, P. v. R.; Li, Q. S. Planar hepta-, octa-, nona-, and decacoordinate first row d-block metals enclosed by boron rings. *Inorg. Chem.* **2009**, *48*, 10679–10686.

39 Miao, C. Q.; Guo, J. C.; Li, S. D. $M@B_9$ and $M@B_{10}$ molecular wheels containing planar nona- and deca-coordinate heavy group 11, 12, and 13 metals (M = Ag, Au, Cd, Hg, In, Tl). *Sci. China, Ser. B: Chem.* **2009**, *52*, 900–904.

40 Averkiev, B. B.; Wang, L. M.; Huang, W.; Wang, L. S.; Boldyrev, A. I. Experimental and theoretical investigations of CB_8^-: Towards rational design of hypercoordinated planar chemical species. *Phys. Chem. Chem. Phys.* **2009**, *11*, 9840–9849.

41 (a) Schleyer, P. v. R.; Maerker, C.; Dransfeld, A.; Jiao, H.; Hommes, N. J. R. v. E. Nucleus-independent chemical shifts: A simple and efficient aromaticity probe. *J. Am. Chem. Soc.* **1996**, *118*, 6317–6318. (b) Chen, Z.; Wannere, C. S.; Corminboeuf, C.; Puchta, R.; Schleyer, P. v. R. Nucleus-independent chemical shifts (NICS) as an aromaticity criterion. *Chem. Rev.* **2005**, *105*, 3842–3888. And its refinement: (c) Fallah-Bagher-Shaidaei, H.; Wannere, C. S.; Corminboeuf, C.; Puchta, R.; Schleyer, P. v. R. Which NICS aromaticity index for planar π rings is best? *Org. Lett.* **2006**, *8*, 863–866.

42 Romanescu, C.; Galeev, T. R.; Li, W. L.; Boldyrev, A. I.; Wang, L. S. Experimental and computational evidence of octa- and nona-coordinated planar iron-doped boron clusters: $Fe©B_8^-$ and $Fe©B_9^-$. *J. Organomet. Chem.* **2012**, *721−722*, 148–154.

43 Wang, L. S. Covalent gold. *Phys. Chem. Chem. Phys.* **2010**, *12*, 8694–8705.

44 Li, W. L.; Romanescu, C.; Piazza, Z. A.; Wang, L. S. Geometric requirements for transition-metal-centered boron wheel clusters: The case of VB_{10}^-. *Phys. Chem. Chem. Phys.* **2012**, *14*, 13663–13669.

45 The electronic design principle can be expressed generally as $x + n + k = (4N_\sigma + 2) + (4N_\pi + 2)$ for double σ- and π-aromaticity. However, we expect that N_σ should be equal to or larger than N_π for truly stable molecular wheels because σ bonding is usually more favorable than π bonding due to better in-plane orbital overlap.

46 Heine, T.; Merino, G. What is the maximum coordination number in a planar structure? *Angew. Chem., Int. Ed.* **2012**, *51*, 4275–4276.

47 Fokwa, B. P. T.; Hermus, M. All-boron planar B_6 ring in the solid-state phase $Ti_7Rh_4Ir_2B_8$. *Angew. Chem., Int. Ed.* **2012**, *51*, 1702–1705.